



## 2:2:1 Resonance in the Quasiperiodic Mathieu Equation

RICHARD RAND

*Department of Theoretical and Applied Mechanics, Cornell University, Ithaca, NY 14853, U.S.A.*

KAMAR GUENNOUN and MOHAMED BELHAQ

*Laboratory of Mechanics, Faculty of Sciences Ain Chock, PB 5366 Maârif, Casablanca, Morocco*

(Received: 9 June 2002; accepted: 7 January 2003)

**Abstract.** In this work, we investigate regions of stability in the vicinity of 2:2:1 resonance in the quasiperiodic Mathieu equation

$$\frac{d^2x}{dt^2} + (\delta + \varepsilon \cos t + \varepsilon\mu \cos(1 + \varepsilon\Delta)t)x = 0,$$

using two successive perturbation methods. The parameters  $\varepsilon$  and  $\mu$  are assumed to be small. The parameter  $\varepsilon$  serves for deriving the corresponding slow flow differential system and  $\mu$  serves to implement a second perturbation analysis on the slow flow system near its proper resonance. This strategy allows us to obtain analytical expressions for the transition curves in the resonant quasiperiodic Mathieu equation. We compare the analytical results with those of direct numerical integration. This work has application to parametrically excited systems in which there are *two* periodic drivers, each with frequency close to twice the frequency of the unforced system.

**Keywords:** Quasiperiodic, Mathieu, subharmonic, resonance.

### 1. Introduction

In this paper, we investigate the transition curves of the quasiperiodic (QP) Mathieu equation in the vicinity of the 2:2:1 resonance. In this case the QP Mathieu equation takes the form

$$\frac{d^2x}{dt^2} + (\delta + \varepsilon \cos t + \varepsilon\mu \cos(1 + \varepsilon\Delta)t)x = 0. \quad (1)$$

Here,  $\varepsilon$  and  $\mu$  are small perturbation parameters, while  $\Delta$  is a frequency detuning parameter.

In a series of papers, Rand and co-workers [1, 2] studied Equation (1) in the case that the driver frequency  $1 + \varepsilon\Delta$  is replaced by a parameter  $\omega$ . They approximated the regions of stability in the  $\delta$ - $\omega$  plane for fixed  $\varepsilon$  by using four different methods: direct numerical integration, Lyapunov exponents, regular perturbations, and harmonic balance. The results obtained by these various techniques were compared and an excellent agreement was obtained. The nonlinear QP Mathieu equation has also been considered [3–5]. Zounes and Rand [3] investigated the interaction of subharmonic resonance bands in a cubic nonlinear QP Mathieu equation using Chirikov's overlap criterion [6] and the analytical machinery presented in [7]. The transition from local chaos to global chaos was investigated. Belhaq and co-workers [4, 5] approximated analytically QP solutions and studied stability of a damped cubic nonlinear QP Mathieu equation, using a double perturbation method. The problem of approximating QP solutions of the original system was then transformed to the study of stationary regimes of the (second) induced autonomous system. Explicit analytical solutions were obtained and

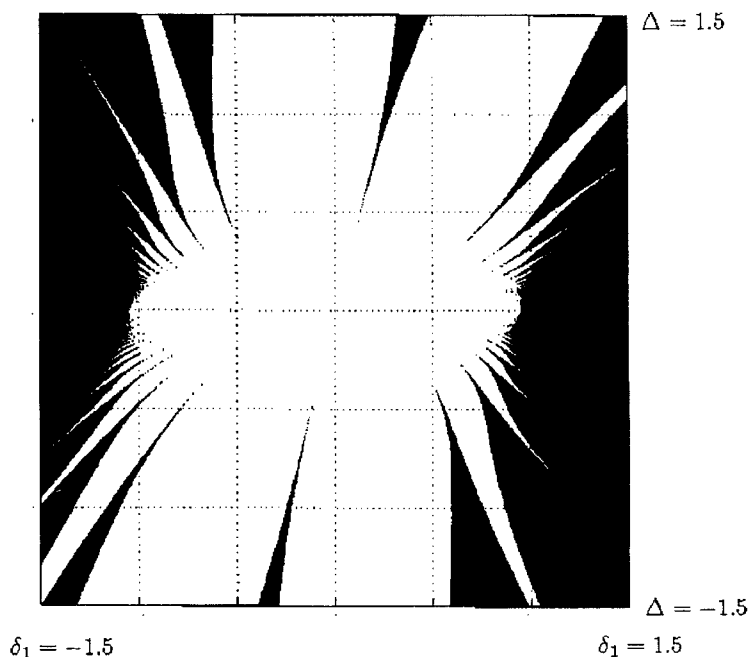


Figure 1. Stability chart of the QP Mathieu equation (1) obtained using numerical integration by Zounes [9] for parameters  $\varepsilon = 0.1$  and  $\mu = 1$ . Here  $\delta = 1/4 + \delta_1 \varepsilon$ . Points in the blackened regions correspond to stable (bounded) motions. Points in the white regions correspond to unstable (unbounded) motions.

good agreement with numerical integrations was shown. For another application of this double perturbation procedure, see [8].

In his Ph.D. thesis, Zounes [9] presented a numerical study of Equation (1) with  $1 + \varepsilon \Delta$  replaced by  $\omega$ . His results included a stability chart which is shown in Figure 1, replotted in the  $\delta_1$ - $\Delta$  parameter plane for  $\varepsilon = 0.1$  and  $\mu = 1$ , where  $\delta = 1/4 + \delta_1 \varepsilon$ . Our goal is to understand this figure through the use of analytical methods. To this end, we apply the double perturbation procedure [4, 5] to determine transition curves in the  $\delta_1$ - $\Delta$  parameter plane. The procedure consists of applying two successive perturbation methods by introducing two small parameter perturbations  $\varepsilon$  and  $\mu$ , such that  $0 < |\varepsilon| \ll |\mu| \ll 1$ . The first reduction is performed using the two variable expansion method associated with  $\varepsilon$ . This leads to a slow flow amplitude-phase system. The second perturbation parameter  $\mu$  which appears in the induced slow flow system allows the application of a second perturbation method, yielding analytical approximations of the transition curves of Equation (1).

## 2. Perturbation Method and Slow Flow System

The two small parameters  $\varepsilon$  and  $\mu$  introduced in Equation (1) allow implementation of two successive perturbation techniques. In the first step we use the two variable expansion method [10] associated with the parameter  $\varepsilon$ . The method consists of introducing two time scales by associating two separate independent variables:  $\xi = t$  and  $\eta = \varepsilon t$ . Substituting these new variables as well as the expressions of the first and second derivatives of  $x$  with respect to

$t$  in term of the new variables, Equation (1) transforms to the following partial differential equation

$$\frac{\partial^2 x}{\partial \xi^2} + 2\varepsilon \frac{\partial^2 x}{\partial \xi \partial \eta} + \varepsilon^2 \frac{\partial^2 x}{\partial \eta^2} + (\delta + \varepsilon \cos \xi + \varepsilon \mu \cos(\xi + \Delta \eta))x = 0. \tag{2}$$

We expand  $x$  and  $\delta$  in power series:

$$x(\xi, \eta; \varepsilon) = x_0(\xi, \eta) + x_1(\xi, \eta)\varepsilon + \dots \tag{3}$$

$$\delta = \frac{1}{4} + \delta_1 \varepsilon + \dots \tag{4}$$

Substituting (3), (4) into (2) and collecting terms gives

$$\frac{\partial^2 x_0}{\partial \xi^2} + \frac{1}{4}x_0 = 0, \tag{5}$$

$$\frac{\partial^2 x_1}{\partial \xi^2} + \frac{1}{4}x_1 = -2 \frac{\partial^2 x_0}{\partial \xi \partial \eta} - \delta_1 x_0 - x_0 \cos \xi - x_0 \mu \cos(\xi + \Delta \eta). \tag{6}$$

We take the solution to Equation (5) in the form

$$x_0 = R(\eta) \cos \left( \frac{\xi}{2} - \theta(\eta) \right). \tag{7}$$

Substituting (7) into (6) and removing secular terms gives

$$\frac{dR}{d\eta} = -\frac{R}{2} [\sin 2\theta + \mu \sin(2\theta + \Delta \eta)], \tag{8}$$

$$\frac{d\theta}{d\eta} = -\delta_1 - \frac{1}{2} [\cos 2\theta + \mu \cos(2\theta + \Delta \eta)]. \tag{9}$$

Note that the parameter  $\mu$  appears in this slow flow system (8), (9) as a new perturbation parameter. Equation (8) has the solution

$$R(\eta) = R(0) \exp \left\{ -\frac{1}{2} \int [\sin 2\theta + \mu \sin(2\theta + \Delta \eta)] d\eta \right\}. \tag{10}$$

Equation (10) will exhibit unbounded solutions if Equation (9) has a limit cycle. The reason is that the integral in (10) will in general not vanish if  $\theta(\eta)$  is a periodic function. On the other hand, all solutions of (10) will be bounded if (9) does not exhibit a limit cycle. In this case the torus flow (9) will be ergodic and the integral in (10) will vanish.

This reasoning leads us to believe that Equation (9) can, to  $O(\varepsilon)$ , determine the stability of the QP Mathieu Equation (1). This is confirmed by numerical simulation of Equation (9), for  $\mu = 1$ , see Figure 2. Comparison with Figure 1, based on Equation (1), for  $\mu = 1$ , shows excellent agreement.

Note that Figure 2 is point-symmetric about  $\delta_1 = 0, \Delta = 0$ , whereas Figure 1 is not. This may be explained by noting that Equation (9) is invariant under the transformation  $\delta_1 \rightarrow -\delta_1, \Delta \rightarrow -\Delta, \theta \rightarrow -\theta + (\pi/2)$ .

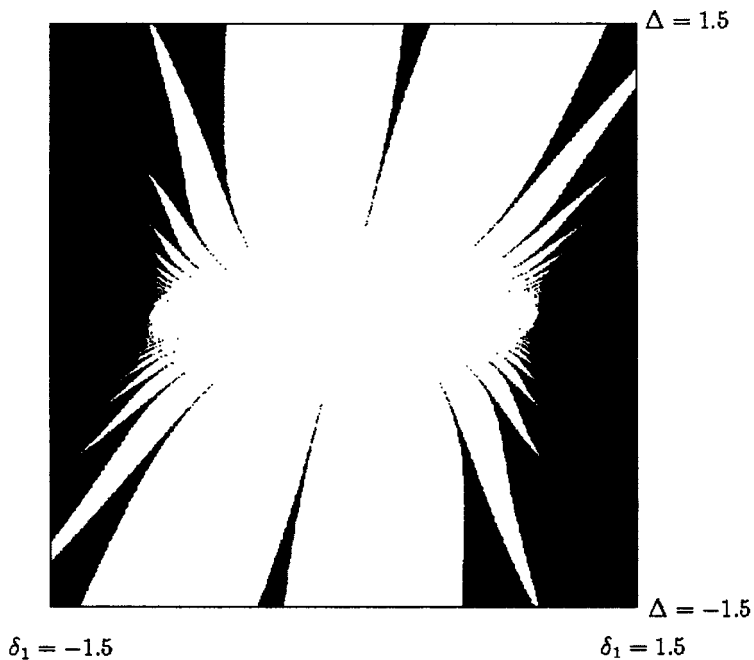


Figure 2. Stability chart obtained by numerically integrating slow flow Equation (9) for  $\mu = 1$ . Points in the blackened regions correspond to absence of limit cycles (stable). Points in the white regions correspond to the presence of limit cycles (unstable). Compare with Figure 1.

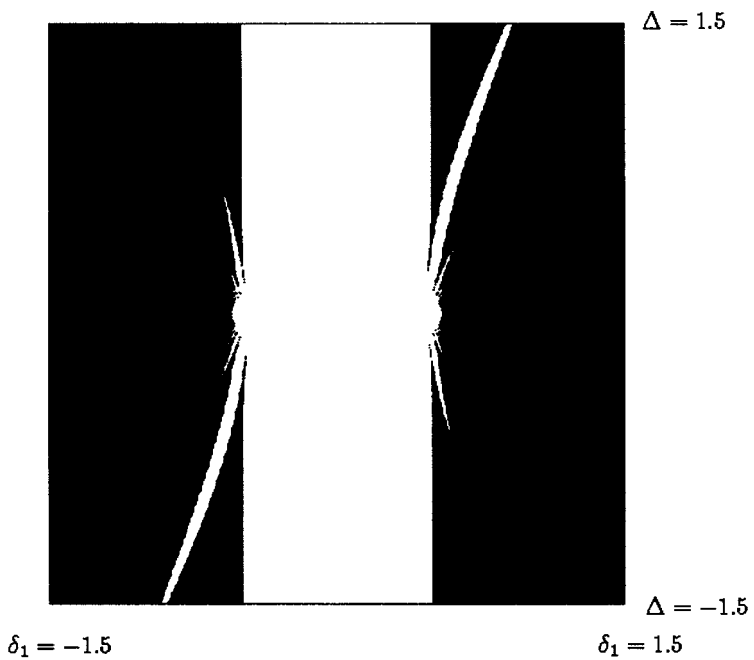


Figure 3. Stability chart obtained by numerically integrating slow flow Equation (9) for  $\mu = 0.1$ . Points in the blackened regions correspond to absence of limit cycles (stable). Points in the white regions correspond to the presence of limit cycles (unstable).

In Figure 3 we present a numerical simulation of Equation (9) for  $\mu = 0.1$ . Note that this figure has many qualitative features in common with Figure 2 (which corresponds to  $\mu = 1$ ). Our goal in this paper is to gain understanding of Figures 1–3 by obtaining analytical expressions for the transition curves separating the regions of stability from those of instability. In order to do so, we will use a second perturbation analysis on the slow flow system (8), (9) for small  $\mu$ .

### 3. Second Perturbation Method and Transition Curves

To begin with, we transform Equations (8), (9) from polar variables  $R, \theta$  to rectangular variables  $A, B$  via the equations:

$$A = R \cos \theta, \quad B = R \sin \theta. \tag{11}$$

This gives

$$\frac{dA}{d\eta} = \left( \delta_1 - \frac{1}{2} \right) B - \mu \frac{A}{2} \sin \Delta\eta - \mu \frac{B}{2} \cos \Delta\eta, \tag{12}$$

$$\frac{dB}{d\eta} = - \left( \delta_1 + \frac{1}{2} \right) A + \mu \frac{B}{2} \sin \Delta\eta - \mu \frac{A}{2} \cos \Delta\eta. \tag{13}$$

We set  $\tau = \Delta\eta$ , whereupon these equations become

$$\Delta \frac{dA}{d\tau} = \left( \delta_1 - \frac{1}{2} \right) B - \mu \frac{A}{2} \sin \tau - \mu \frac{B}{2} \cos \tau, \tag{14}$$

$$\Delta \frac{dB}{d\tau} = - \left( \delta_1 + \frac{1}{2} \right) A + \mu \frac{B}{2} \sin \tau - \mu \frac{A}{2} \cos \tau. \tag{15}$$

We treat these equations by algebraically eliminating  $B$ , giving a single second order o.d.e. on  $A$ . To do this, we differentiate (14) with respect to  $\tau$  and then substitute  $dB/d\tau$  from (15). Finally we solve (14) for  $B$  and substitute the result. This gives an equation which may be written in the form

$$\frac{d^2A}{d\tau^2} + f_1(\tau) \frac{dA}{d\tau} + f_2(\tau)A = 0, \tag{16}$$

where  $f_1(\tau)$  and  $f_2(\tau)$  are  $2\pi$ -periodic functions and where

$$f_1(\tau) = O(\mu) \quad \text{and} \quad f_2(\tau) = \left( \frac{\delta_1^2 - \frac{1}{4}}{\Delta^2} \right) + O(\mu). \tag{17}$$

Next we construct analytic expressions for the transition curves in  $\delta_1$ - $\Delta$  parameter plane which separate stable (bounded) solutions from unstable (unbounded) solutions. From Floquet theory, we know that on these transition curves there exist periodic solutions with period  $2\pi$  or  $4\pi$ , since the period of the coefficients  $f_1$  and  $f_2$  is  $2\pi$ . Thus we follow Stoker [11] and seek a solution to (16) in the form of a Fourier series with period  $4\pi$  (which includes period  $2\pi$  as a special case):

$$A(\tau) = \sum_{n=0}^{\infty} c_n \cos \frac{n\tau}{2} + d_n \sin \frac{n\tau}{2}. \tag{18}$$

We substitute (18) into (16) and collect terms. This work is algebraically intensive and was done on MACSYMA. There result four sets of algebraic equations on the coefficients  $c_n$  and  $d_n$ . Each set deals exclusively with  $c_{\text{even}}$ ,  $d_{\text{even}}$ ,  $c_{\text{odd}}$  and  $d_{\text{odd}}$ , respectively. Each set is homogenous and of infinite order, so for a nontrivial solution the determinant must vanish. This gives four infinite determinants. For brevity we omit showing these here. We find that in the unperturbed autonomous case,  $\mu = 0$ , these determinants have the following roots:

$$\Delta = \frac{\sqrt{4\delta_1^2 - 1}}{N}, \quad N = 1, 2, 3, \dots \tag{19}$$

Equation (19) represents resonance conditions between the  $\mu = 0$  slow flow oscillator given in Equations (14), (15), and the slow flow forcing functions  $\sin \Delta\eta$ ,  $\cos \Delta\eta$ . In order to obtain expressions for the associated transition curves, we detune these resonances:

$$\Delta = \frac{\sqrt{4\delta_1^2 - 1}}{N} + \mu\sigma_1 + \mu^2\sigma_2 + \dots, \quad N = 1, 2, 3, \dots, \tag{20}$$

where the detuning constants  $\sigma_i$  are as yet unknown. We substitute Equation (20) into each of the four vanishing determinants, expand in  $\mu$ , collect terms and solve for the unknown constants  $\sigma_i$ . Here are the first two transition curves obtained in this way:

$$\begin{aligned} \Delta = & \sqrt{4\delta_1^2 - 1} \pm \frac{(2\delta_1 \sqrt{4\delta_1^2 - 1} + 4\delta_1^2 - 1) \mu}{8\delta_1^2 - 2} \\ & - \frac{((8\delta_1^2 - 1) \sqrt{4\delta_1^2 - 1} - 16\delta_1^3 + 4\delta_1) \mu^2}{256\delta_1^4 - 128\delta_1^2 + 16} + \dots, \end{aligned} \tag{21}$$

$$\Delta = \frac{\sqrt{4\delta_1^2 - 1}}{2} - \frac{((4\delta_1 + 3) \sqrt{4\delta_1^2 - 1} + 16\delta_1^2 - 5) \mu^2}{\sqrt{4\delta_1^2 - 1} (48\delta_1^2 - 12)} + \dots \tag{22}$$

Note that these expressions are singular in the neighborhood of  $\delta_1 = \pm 1/2$ . Nevertheless, these expressions compare favorably with the numerical results shown in Figure 3 (see Figure 4 where the first eight transition curves are displayed).

#### 4. Discussion

The analytical methods presented in this work offer an explanation of the nature of the stability chart shown in Figures 1–3 which may be expressed in words, as follows. For small values of  $\mu$ , the expressions for the transition curves given by Equations (21), (22) require that  $|\delta_1| > 1/2$ . This means that the  $\cos t$  driver in Equation (1) is too detuned off of 2:1 resonance with the unforced oscillator to produce instability. (This follows from the fact that in the usual Mathieu equation, Equation (1) with  $\mu = 0$ , the 2:1 transition curves have the well-known expression  $\delta = 1/4 \pm \varepsilon/2 + O(\varepsilon^2)$ .) Thus the instability associated with the transition curves (21), (22) cannot come from 2:1 resonance with the  $\cos t$  driver, and must have some other source. The resulting motion, if  $\mu = 0$ , would be a QP motion with frequencies 1 coming from the  $\cos t$  driver, and  $\sqrt{\delta_1^2 - (1/4)}$ , which is the slow flow frequency of the slow time modulating functions  $A(\eta)$ ,  $B(\eta)$ , see Equations (12), (13). Now if  $\mu \neq 0$ , another resonance

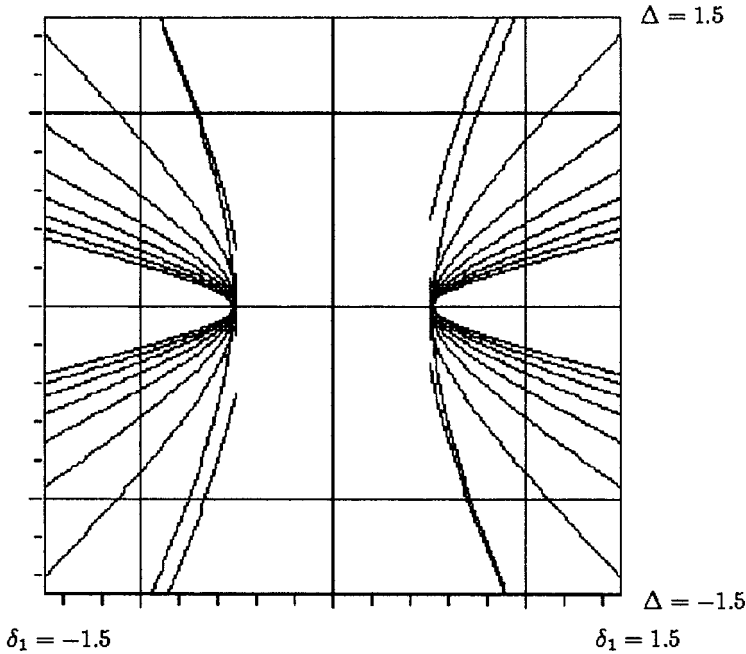


Figure 4. Transition curves, as obtained from double-perturbation procedure for  $\mu = 0.1$ . Compare with Figure 3.

can occur between the  $A(\eta)$ ,  $B(\eta)$ ,  $\mu = 0$  oscillator, which runs with slow flow frequency  $\sqrt{\delta_1^2 - (1/4)}$ , and the slow flow driver,  $\sin \Delta\eta$ ,  $\cos \Delta\eta$ , which runs at slow flow frequency  $\Delta$ . This latter frequency is seen to be the difference between the two drivers in the original QP Mathieu Equation (1), and may be thought of as the extent of the drift of the  $\cos(1 + \varepsilon\Delta)t$  driver relative to the  $\cos t$  driver. The order of the superharmonic tells how many cycles the slow flow  $A$ ,  $B$  oscillator goes through in one cycle of the frequency  $\Delta$  slow flow driver during instability, that is, the order of the resonance. Thus we may conclude that each of the white instability regions in Figures 1–3 corresponds to a distinct order of resonance between the  $\mu = 0$  slow flow motion and the frequency of drift between the two drivers in Equation (1).

### 5. Conclusion

In this work, we have constructed analytical expressions for the transition curves of the QP Mathieu equation in the vicinity of the resonance 2:2:1. A double-perturbation procedure was applied to obtain the analytical approximations to these transition curves. In a first step, we have applied the two variable expansion method to the QP Mathieu equation and derived the slow flow system. To obtain expressions for the transition curves we have implemented another perturbative study near the proper resonance of the slow flow system. The analytical expressions obtained by this procedure show a good agreement with the direct numerical integration of the original QP Mathieu equation. Moreover, the results from the perturbation expansions were used to draw qualitative conclusions regarding the structure of Figures 1–3. It was shown that each of the white instability regions in Figures 1–3 corresponds to a distinct order of resonance between the  $\mu = 0$  slow flow motion and the frequency of drift between the two drivers in Equation (1).

## References

1. Rand, R., Zounes, R., and Hastings, R., 'Dynamics of a quasiperiodically forced Mathieu oscillator', in *Non-Linear Dynamics: The Richard Rand 50th Anniversary Volume*, A. Guran (ed.), World Scientific, Singapore, 1997, pp. 203–221.
2. Zounes, R. and Rand, R., 'Transition curves for the quasiperiodic Mathieu equation', *SIAM Journal on Applied Mathematics* **58**, 1998, 1094–1115.
3. Zounes, R. and Rand, R., 'Global behavior of a nonlinear quasiperiodic Mathieu equation', *Nonlinear Dynamics* **27**, 2002, 87–105.
4. Belhaq, M., Guennoun, K., and Houssni, M., 'Asymptotic solutions for a damped non-linear quasi-periodic Mathieu equation', *International Journal of Non-Linear Mechanics* **37**, 2002, 445–460.
5. Guennoun, K., Houssni, M., and Belhaq, M., 'Quasi-periodic solutions and stability for a weakly damped nonlinear quasiperiodic Mathieu equation', *Nonlinear Dynamics* **27**, 2002, 211–236.
6. Chirikov, B. V., 'A universal instability of many-dimensional oscillator systems', *Physics Reports* **52**, 1979, 263–379.
7. Zounes, R. and Rand, R., 'Subharmonic resonance in the nonlinear Mathieu equation', *International Journal of Non-Linear Mechanics* **37**, 2002, 43–73.
8. Belhaq, M. and Houssni, M., 'Quasiperiodic oscillations, chaos and suppression of chaos in a nonlinear oscillator driven by parametric and external excitations', *Nonlinear Dynamics* **18**, 1999, 1–24.
9. Zounes, R., 'An analysis of the nonlinear quasiperiodic Mathieu equation', Ph.D. Dissertation, Center for Applied Mathematics, Cornell University, Ithaca, NY, 1997.
10. Bender, C. M. and Orszag, S. A., *Advanced Mathematical Methods for Scientists and Engineers*, McGraw-Hill, New York, 1978.
11. Stoker, J. J., *Nonlinear Vibrations in Mechanical and Electrical Systems*, Wiley, New York, 1950.